

## Subcortical volumes as early predictors of fatigue in multiple sclerosis

Vinzenz Fleischer, Dumitru Ciolac, Gabriel Gonzalez Escamilla, Matthias Grothe, Sebastian Strauss, Lara S. Molina Galindo, Angela Radetz, Anke Salmen, Carsten Lukas, Luisa Klotz, Sven G. Meuth, Antonios Bayas, Friedemann Paul, Hans Peter Hartung, Christoph Heesen, Martin Stangel, Brigitte Wildemann, Florian Then Bergh, Björn Tackenberg, Tania Kümpfel, Uwe K. Zettl, Matthias Knop, Hayrettin Tumani, Heinz Wiendl, Ralf Gold, Stefan Bittner, Frauke Zipp, Sergiu Groppa, Muthuraman Muthuraman

### Angaben zur Veröffentlichung / Publication details:

Fleischer, Vinzenz, Dumitru Ciolac, Gabriel Gonzalez Escamilla, Matthias Grothe, Sebastian Strauss, Lara S. Molina Galindo, Angela Radetz, et al. 2022. "Subcortical volumes as early predictors of fatigue in multiple sclerosis." *Annals of Neurology* 91 (2): 192–202. <https://doi.org/10.1002/ana.26290>.

# Subcortical Volumes as Early Predictors of Fatigue in Multiple Sclerosis

Vinzenz Fleischer, MD,<sup>1</sup> Dumitru Ciolac, MD ,<sup>1</sup> Gabriel Gonzalez-Escamilla, PhD,<sup>1</sup> Matthias Grothe, MD,<sup>2</sup> Sebastian Strauss, MD,<sup>2</sup> Lara S. Molina Galindo, MD,<sup>1</sup> Angela Radetz, PhD,<sup>1</sup> Anke Salmen, MD,<sup>3,4</sup> Carsten Lukas, MD ,<sup>3</sup> Luisa Klotz, MD,<sup>5</sup> Sven G. Meuth, MD, PhD,<sup>5,6</sup> Antonios Bayas, MD,<sup>7</sup> Friedemann Paul, MD ,<sup>8</sup> Hans-Peter Hartung, MD ,<sup>6</sup> Christoph Heesen, MD,<sup>9</sup> Martin Stangel, MD ,<sup>10</sup> Brigitte Wildemann, MD,<sup>11</sup> Florian Then Bergh, MD,<sup>12</sup> Björn Tackenberg, MD,<sup>13,14</sup> Tania Kümpfel, MD ,<sup>15</sup> Uwe K. Zettl, MD,<sup>16</sup> Matthias Knop, MD,<sup>17</sup> Hayrettin Tumani, MD,<sup>18</sup> Heinz Wiendl, MD,<sup>5</sup> Ralf Gold, MD,<sup>3</sup> Stefan Bittner, MD,<sup>1</sup> Frauke Zipp, MD ,<sup>1</sup> Sergiu Groppa, MD,<sup>1</sup> Muthuraman Muthuraman, PhD, <sup>1</sup> and the German Competence Network Multiple Sclerosis (KKNMS)

**Objective:** Fatigue is a frequent and severe symptom in multiple sclerosis (MS), but its pathophysiological origin remains incompletely understood. We aimed to examine the predictive value of subcortical gray matter volumes for fatigue severity at disease onset and after 4 years by applying structural equation modeling (SEM).

**Methods:** This multicenter cohort study included 601 treatment-naïve patients with MS after the first demyelinating event. All patients underwent a standardized 3T magnetic resonance imaging (MRI) protocol. A subgroup of 230 patients with available clinical follow-up data after 4 years was also analyzed. Associations of subcortical volumes (included into SEM) with MS-related fatigue were studied regarding their predictive value. In addition, subcortical regions that have a central role in the brain network (hubs) were determined through structural covariance network (SCN) analysis.

View this article online at [wileyonlinelibrary.com](https://onlinelibrary.wiley.com/doi/10.1002/ana.26290). DOI: 10.1002/ana.26290

Received Jun 23, 2021, and in revised form Dec 22, 2021. Accepted for publication Dec 22, 2021.

Address correspondence to Dr Vinzenz Fleischer, Department of Neurology, Focus Program Translational Neuroscience (FTN), Rhine-Main-Neuroscience (rmn), Johannes Gutenberg-University Mainz, Langenbeckstr. 1, 55131 Mainz, Germany. E-mail: [vinzenz.fleischer@unimedizin-mainz.de](mailto:vinzenz.fleischer@unimedizin-mainz.de)

Muthuraman Muthuraman, Department of Neurology, Focus Program Translational Neuroscience (FTN), Rhine-Main-Neuroscience (rmn), Johannes Gutenberg-University Mainz, Langenbeckstr. 1, 55131 Mainz, Germany. E-mail: [mmuthura@uni-mainz.de](mailto:mmuthura@uni-mainz.de)

Sergiu Groppa and Muthuraman Muthuraman are senior authors and contributed equally to this work.

[Correction added on February 10, 2022, after first online publication: Muthuraman Muthuraman has been included as one of the Corresponding author.]

From the <sup>1</sup>Department of Neurology, Focus Program Translational Neuroscience (FTN) and Immunotherapy (FZI), Rhine Main Neuroscience Network (rmn<sup>2</sup>), University Medical Center of the Johannes Gutenberg University Mainz, Mainz, Germany; <sup>2</sup>Department of Neurology, University Medicine of Greifswald, Greifswald, Germany; <sup>3</sup>Department of Neurology, St. Josef-Hospital, Ruhr-University Bochum, Bochum, Germany; <sup>4</sup>Department of Neurology, Inselspital, Bern University Hospital and University of Bern, Bern, Switzerland; <sup>5</sup>Department of Neurology, University Hospital Münster, Westfälische-Wilhelms-University Münster, Münster, Germany; <sup>6</sup>Department of Neurology, University of Duesseldorf, Duesseldorf, Germany; <sup>7</sup>Department of Neurology, University Hospital Augsburg, Augsburg, Germany; <sup>8</sup>NeuroCure Clinical Research Center and Experimental and Clinical Research Center, Charité, Universitätsmedizin Berlin and Max Delbrueck Center for Molecular Medicine, Berlin, Germany; <sup>9</sup>Institute for Neuroimmunology and Multiple Sclerosis, Universitätsklinikum Hamburg-Eppendorf, Hamburg, Germany; <sup>10</sup>Clinical Neuroimmunology and Neurochemistry, Department of Neurology, Hannover Medical School, Hannover, Germany; <sup>11</sup>Department of Neurology, University of Heidelberg, Heidelberg, Germany; <sup>12</sup>Department of Neurology, University of Leipzig, Leipzig, Germany; <sup>13</sup>Department of Neurology, Philipps-University Marburg, Marburg, Germany; <sup>14</sup>F. Hoffmann-La Roche AG, Basel, Switzerland; <sup>15</sup>Institute of Clinical Neuroimmunology, Ludwig Maximilian University of Munich, Munich, Germany; <sup>16</sup>Department of Neurology, Neuroimmunological Section, University of Rostock, Rostock, Germany; <sup>17</sup>Max Planck Institute of Psychiatry, Munich, Germany; and <sup>18</sup>Department of Neurology, University of Ulm, Ulm, Germany

Additional supporting information can be found in the online version of this article.

192 © 2021 The Authors. *Annals of Neurology* published by Wiley Periodicals LLC on behalf of American Neurological Association.

This is an open access article under the terms of the Creative Commons Attribution-NonCommercial-NoDerivs License, which permits use and distribution in any medium, provided the original work is properly cited, the use is non-commercial and no modifications or adaptations are made.

**Results:** Predictive causal modeling identified volumes of the caudate ( $s$  [standardized path coefficient] = 0.763,  $p = 0.003$  [left];  $s = 0.755$ ,  $p = 0.006$  [right]), putamen ( $s = 0.614$ ,  $p = 0.002$  [left];  $s = 0.606$ ,  $p = 0.003$  [right]) and pallidum ( $s = 0.606$ ,  $p = 0.012$  [left];  $s = 0.606$ ,  $p = 0.012$  [right]) as prognostic factors for fatigue severity in the cross-sectional cohort. Moreover, the volume of the pons was additionally predictive for fatigue severity in the longitudinal cohort ( $s = 0.605$ ,  $p = 0.013$ ). In the SCN analysis, network hubs in patients with fatigue worsening were detected in the putamen ( $p = 0.008$  [left];  $p = 0.007$  [right]) and pons ( $p = 0.0001$ ).

**Interpretation:** We unveiled predictive associations of specific subcortical gray matter volumes with fatigue in an early and initially untreated MS cohort. The colocalization of these subcortical structures with network hubs suggests an early role of these brain regions in terms of fatigue evolution.

ANN NEUROL 2022;91:192–202

Multiple sclerosis (MS) is a chronic immune-mediated disease of the central nervous system characterized by inflammation, demyelination, and neurodegeneration.<sup>1</sup> Beyond clinical relapses and neurological impairment, up to 80% of patients suffer from fatigue during the course of the disease, which heavily impacts social, cognitive, and physical functioning and leads to reduced health-related quality of life.<sup>2,3</sup> Despite this high prevalence, studies on fatigue have long been neglected in MS research due to the multifaceted aspect of fatigue comprising a constellation of motor, cognitive, and mood performance.<sup>4</sup>

Fatigue also appears to be frequently present in the earliest stages of the disease,<sup>2</sup> including in patients with a clinically isolated syndrome (CIS) or radiologically isolated syndrome (RIS), and is associated with a greater risk of converting to clinically definite MS, arguing for a prognostic value of fatigue.<sup>5</sup> Recent evidence even endorses the existence of a prodromal fatigue period suggesting that fatigue can even start years before clinical manifestations.<sup>6,7</sup>

Magnetic resonance imaging (MRI) has been used to explore structural and functional correlates of fatigue. Although fatigue is associated with clinical disability, structural imaging studies revealed inconsistent results regarding the relationship between fatigue severity and structural MRI correlates (eg, lesion load).<sup>8</sup> However, the atrophy of several brain regions including frontal cortex,<sup>9</sup> posterior parietal cortex,<sup>10</sup> and thalamus<sup>11</sup> were shown to be anatomic correlates of fatigue as were global measures of atrophy.<sup>12</sup> In addition, several studies emphasized widespread damage of the normal-appearing white matter in patients with fatigue.<sup>13</sup>

The relationship between functional MRI abnormalities and MS-related fatigue has been consistently proven, both in task-related<sup>14,15</sup> and resting state<sup>16,17</sup> functional MRI studies. These studies revealed abnormally high activity and functional connectivity in brain regions of the sensorimotor network, the insula, the prefrontal cortex, the cerebellum, and the basal ganglia, correlating with individual fatigue severity.<sup>18</sup> Thus, functional integration among the cerebral cortex and subcortical structures, such as basal ganglia, thalamus, and cerebellum, seems to be an important scaffold in MS-related fatigue.<sup>18–20</sup> These observations support the hypothesis that MS-related

fatigue is associated with functional reorganization, which seems to occur mainly through a dysfunction of striato-cortical circuits.<sup>21,22</sup> Hence, fatigue-related atrophy functionally spreads beyond the sites of structural injury into widely interconnected regions and evidently rearranges the entire structural and functional brain network.<sup>23</sup>

However, the exact spatial distribution pattern of subcortical brain volumes at disease onset and its relation to the development of fatigue is poorly understood. The goal of this study was to unravel the relationship between fatigue and its structural determinants after the first demyelinating event, and to make prognostic inferences from these regarding fatigue severity within a large cohort of treatment-naïve patients with MS patients. For clinical decision making, it is important to obtain the earliest possible prognostic factors that predict fatigue worsening, because early immunotherapeutic treatment does not only influence the neurological outcome in terms of physical disability, but also positively MS-related fatigue.<sup>24</sup>

Here, fatigue was measured in a prospective, multicenter cohort study of patients with early MS at disease onset ( $n = 601$ ) and after 4-year follow-up ( $n = 230$ ). Within the statistical framework of predictive modeling, we applied structural equation models (SEM) to brain MRI-derived subcortical volumes that best predicted fatigue in patients after the first demyelinating event. Finally, structural covariance network (SCN) analysis was applied to the subcortical volumes to account for the spatial complexity of tissue damage on a network level. Thereby, brain network hubs were determined to identify regions occupying a central network position in the brain of patients with MS with progressing fatigue.

## Methods

### Participants

The German National MS (NationMS) cohort is a multicenter prospective longitudinal observational study comprising detailed assessment of patients with first diagnosis of relapsing-remitting MR (RRMS) or CIS. All participating centers belong to the nationwide German Competence Network Multiple Sclerosis (KKNMS). Patients were recruited at 15 neurological tertiary referral centers in Germany.

Patients with initial diagnosis of either CIS<sup>25</sup> or RRMS (according to the revised McDonald diagnostic criteria)<sup>26</sup> without any prior immunomodulatory treatment were prospectively recruited. After satisfying the study's inclusion criteria,<sup>27</sup> patients were comprehensively examined and observed for a 4-year follow-up period according to a standardized assessment plan outlined elsewhere.<sup>2</sup> Of the 1,123 patients enrolled, baseline 3T MRI datasets were available for 845 patients; 601 patients had complete baseline clinical scores and were finally included into the analysis (baseline cohort). In the subcohort, 335 patients completed the 4-year follow-up with clinical scores available for 230 patients that were included into the longitudinal analysis (4-year follow-up cohort). Furthermore, 89 healthy individuals without a neurological disease were included with 3T MRI datasets and fatigue scores available. Written informed consent in accordance with the Declaration of Helsinki was obtained from all subjects before participation; the study was approved by the Ethics Committee of Ruhr-University Bochum (registration no. 3714-10), and consecutively by all local committees of the participating centers.

### Clinical Assessment

Each patient was clinically assessed by an experienced neurologist and the Expanded Disability Status Scale (EDSS) score was determined at disease onset (study entrance) and after 4 years. Fatigue was measured with 2 neuropsychological instruments applied in MS studies: the Fatigue subscale as part of the "Multiple Sclerosis Inventory of Cognition" (MUSIC)<sup>28</sup> used as a brief neurocognitive screening instrument and the more common and established "Fatigue Scale for Motor and Cognitive Functions" (FSMC)<sup>29</sup> used in the diagnostic set-up as well as in the regular clinical follow-up.

The MUSIC test was developed as a screening tool to evaluate neurocognitive dysfunction comprising 5 subscales, including one subscale assessing fatigue. For fatigue evaluation, MUSIC includes 3 items, each using a rating scale from 1 (completely wrong) to 7 (completely true), yielding a maximum score of 21 points. The FSMC represents a more advanced patient self-reported questionnaire, which consists of 20 questions and evaluates in more detail the motor and cognitive components of the fatigue. Currently, the FSMC tool is recommended for a multidimensional approach to reliably assess fatigue in patients with MS.<sup>30</sup>

To control fatigue for overlapping depressive symptoms, depression was assessed using the Beck Depression Inventory-II (BDI-II), which consists of 21 items that assess affective, cognitive, and somatic symptoms of depression.<sup>31</sup>

### MRI Acquisition

Conventional MRI images were acquired at different 3T scanners with a 32-channel receive-only head coil, according to a standardized imaging protocol in all centers. This protocol included sagittal 3D T1-weighted magnetization prepared rapid acquisition of gradient echo (MP-RAGE) and T2-weighted fluid-attenuated inversion recovery (FLAIR) sequences. MP-RAGE acquisition parameters: repetition time (TR) = 1900 ms, echo time (TE) = 2.52 ms, inversion time (TI) = 900 ms, flip angle (FA) = 9°, matrix size = 256 × 256, field of view (FOV) = 256 × 256 mm<sup>2</sup>, slice thickness (ST) = 1 mm, voxel size (VS) = 1 × 1 × 1 mm<sup>3</sup>; FLAIR acquisition parameters: TR = 5,000 ms, TE = 388 ms, TI = 1800 ms, matrix size = 256 × 256, FOV = 256 × 256 mm<sup>2</sup>, ST = 1 mm, and VS = 1 × 1 × 1 mm<sup>3</sup>.

### Lesion Filling

The structural MRI datasets of all patients were collected and processed in one analyzing center (Mainz). Initially, lesion maps were drawn on T2-weighted 3D FLAIR images using the MRIcron software (<http://www.mccauslandcenter.sc.edu>). Using the lesion segmentation toolbox (LST), which is part of the statistical parameter mapping (SPM8) software, 3D FLAIR images were co-registered to 3D-T1 images and bias corrected. After partial volume estimation, lesion segmentation was performed with 20 different initial threshold values for the lesion growth algorithm.<sup>32</sup> By comparing automatically and manually estimated lesion maps, the optimal threshold ( $\kappa$  value, dependent on image contrast) was determined for each patient and an average value for all patients was calculated. Afterward, for automatic lesion volume estimation and filling of 3D-T1 images, a uniform  $\kappa$  value of 0.1 was applied in all patients. Subsequently, the filled 3D-T1 images as well as the native 3D-T1 images were segmented into gray matter (GM), white matter (WM), and cerebrospinal fluid (CSF) and normalized to MNI space. Finally, the quality of the segmentations was visually inspected. Lesion-filled native T1-weighted images were used for the computation based on regional GM properties.

### Cortical and Subcortical Volume Analysis

FreeSurfer image analysis suit (version 6.0, <http://surfer.nmr.mgh.harvard.edu/>) was used for cortical surface reconstruction and subcortical volume segmentation from T1-weighted images in a fully automated fashion, followed by visual inspection for quality control at various processing steps. Technical details of processing stream for surface-based reconstruction are described elsewhere.<sup>33</sup> In summary, the surface-based processing stream consists of skull stripping, Talairach space transformation, optimization of GM-WM and GM-CSF boundaries, segmentation

of subcortical WM, and deep GM (DGM) structures and tessellation.<sup>33</sup> Afterward, the cerebral cortex and subcortical structures were divided into 89 anatomic labels corresponding to the Desikan-Kiliany and Harvard-Oxford atlases (Supplemental Table S1).<sup>34</sup> The extracted volumes were subsequently used to construct predictive models through SEM (see SEM analysis) and, in addition, to create a covariance matrix for the structural covariance network analysis (see Structural covariance network reconstruction).

### **SEM: Model Construction**

The SEM analysis was performed in SEM toolbox for MATLAB (version 13a; Mathworks, Natick, MA, USA). SEM represents a complex analytical tool that can determine the causal relationships between the variables in a model-based approach. In the first model, the relationship between brain structures (ie, volumes of basal ganglia, brain stem, and cerebellum) and clinical scores (fatigue scores derived from MUSIC and FSMC tests and EDSS) at baseline in 601 patients were assessed. In the second model, the relationship between the above-mentioned subcortical volumes and clinical variables at baseline and at 4-year follow-up in 230 patients was investigated. Finally, within the third (cross-sectional) and fourth models (longitudinal), we explored the association between demographical (age and sex) and clinical variables (MUSIC, FSMC, and EDSS).

### **SEM: Parameter Estimation**

We used the Maximum Likelihood method of estimation to fit the models. In order to adjust the models for a large sample size, we used the Root Mean Square Error of Approximation (RMSEA) index, which improves precision without increasing bias.<sup>35</sup> The RMSEA index estimates lack of fit in a model compared to a perfect model and therefore should be low. In all models, the Invariant under a Constant Scaling (ICS) and ICS factor (ICSF) criteria should be close to zero, indicating that models were appropriate for analysis. Finally, based on the Akaike Information Criterion (AIC) the quality of each model relative to other models was estimated, with smaller values signifying a better fit of the model. The strength of associations between the variables in the models was quantified by standardized coefficients ( $s$ ), ranging from 0 (no association) to 1 (very strong association). The  $p$  values of  $< 0.05$  were considered statistically significant.

### **Structural Covariance: Network Reconstruction**

Individual cortical and subcortical volume values were obtained for each region of interest to construct covariance matrices ( $N \times N$ ), where  $N$  is the number of regions of

interest.<sup>36</sup> Hence, the covariance matrix depicts the summary of all pairwise associations (connections) between brain regions (network nodes). To generate group-level network covariance matrices, patients were stratified into 2 groups based on whether they progressed over the 4 year of follow-up or not. Both fatigue (MUSIC and FSMC) and disability (EDSS) progression were defined as higher scores at follow-up in comparison to the corresponding baseline scores (difference between baseline and follow-up), as previously described.<sup>37</sup> Unchanged or lower scores at follow-up were considered stable. Overall, worsening was observed in 105 patients with MS in the MUSIC score (125 no MUSIC progression), 133 in the FSMC score (97 no FSMC progression) and 93 in the EDSS score (137 no EDSS progression).

The structural correlation matrices ( $89 \times 89$ ) for each group contained the Pearson's correlation coefficient between the cortical and subcortical volumes of each pair of regions. To describe the topological organization of the derived structural networks, network measures (see below) were obtained using weighted matrices in the Graph Analysis Toolbox (GAT) toolbox,<sup>38</sup> which is a MATLAB-based software providing nonparametric statistics for comparing regional topology and network hubs between groups.<sup>39</sup>

### **Structural Covariance: Network Characterization**

Accordingly, the resulting matrices were fed into the graph theoretical analysis for the mathematical description and quantification of the structural network topology, with emphasis on the detection of hub regions. Hubs are nodes (the predefined regions based on the above-mentioned atlas) occupying a central position in the overall organization of a network, generally characterized by their high degree of connectivity to other regions.<sup>40</sup> Hubs can be detected using numerous different graph measures. Here, hub identification was based on the computation of a centrality measure called betweenness centrality. Betweenness centrality expresses the number of short paths that a node (brain region) participates in. Ref.39 These hubs were determined as those nodes, whose betweenness centrality was at least  $\pm 2$  standard deviations away from the mean betweenness centrality of all regions. A high level of centrality of hubs represents nodes that are less vulnerable and susceptible to disconnection and dysfunction in the brain.<sup>40</sup> The reported  $p$  values were corrected using the false discovery rate (FDR) approach in order to remain statistically conservative.<sup>41</sup>

### **Statistical Analysis**

Statistical analyses of the demographic and clinical data were performed using SPSS 23 software (SPSS, Chicago,

IL, USA). Frequencies and means are reported for categorical and continuous variables, respectively (the Table). All variables were checked for normality using the Shapiro–Wilk test and histogram inspection. Fatigue scores derived from MUSIC and FSMC between baseline and 4-year follow-up were compared using a paired *t* test. A Wilcoxon signed-rank test was used to assess longitudinal changes in EDSS. Group comparison *p* values < 0.05 were considered statistically. Unless otherwise indicated, data are expressed as mean ± SD (standard deviation).

## Results

### Clinical Characteristics of the Study Cohorts

At baseline, of 601 patients (424 women [71%] / 177 men [29%]; mean age ± SD: 33.8 ± 9.7 years; median EDSS [range]: 1.5 [0–5.0]), 256 (43%) were diagnosed with CIS and 345 (57%) patients already had definite RRMS. The mean disease duration was 7.3 ± 11.8 months (see Table).

From the 601 patients, 230 were clinically followed-up for 4 years. This 4-year follow-up cohort included 155 (67%) women and 75 (33%) men with a mean age of 35.4 ± 10.1 years (median EDSS 1.5 [0–6.0]). After the 4-year follow-up, 77 of 100 patients (77%) who were initially diagnosed with CIS had converted to RRMS. After the first demyelinating event, 44% of the patients started a disease-modifying treatment.

At 4-year follow-up, all patients presented significantly higher scores of fatigue assessed by the FSMC test (paired *t* test = −4.3, *p* < 0.001), whereas the MUSIC screening test did not significantly change over the observation time (paired *t* test = −1.7, *p* = 0.082) compared to the values obtained at baseline. The EDSS score significantly changed over the 4 years of follow-up (Wilcoxon signed-ranks test [*Z*] = 2.2, *p* = 0.029).

### Robustness of the Models

In the predictive modeling approach, the RMSEA index for all models was below 0.03 and the AIC comparing the models varied between 0.008 and 0.029 (Supplementary Table S2). Hence, the obtained fit indices in the SEM analysis implied a good fit of the constructed models to the observed data, providing robust causal relations between the variables.<sup>42</sup>

### Subcortical Volumes Associate with Fatigue and Clinical Impairment

In the 601 treatment-naïve patients with CIS and RRMS, the baseline fatigue scores measured by MUSIC and FSMC were strongly associated with the volumes of bilateral caudate and putamen (Figs 1 and 2A) in the first SEM model. Right thalamus and left hippocampus were also independently associated with both fatigue scores at disease onset by showing a significant association with FSMC and MUSIC (see Figs 1 and 2A), whereas

**TABLE. Study Cohort**

| Clinical data                           | Baseline cohort (n = 601) | 4-year follow-up cohort (n = 230) |                          |
|---|---------------------------|-----------------------------------|--------------------------|
| Sex, female/male                        | 424/177                   | 155/75                            |                          |
| MS subtype at baseline, CIS/RRMS        | 256/344                   | 100/130                           |                          |
| Mean age at disease onset (± SD), years | 33.2 ± 9.7                | 34.8 ± 10.1                       |                          |
| Mean age at baseline MRI (± SD), years  | 33.8 ± 9.7                | 35.4 ± 10.1                       |                          |
| Mean disease duration (± SD), months    | 7.3 ± 11.8                | 6.8 ± 7.0                         |                          |
| Mean fatigue, MUSIC (± SD)              | 7.1 ± 4.3                 | 7.7 ± 4.6 <sup>a</sup>            | 8.4 ± 5.3 <sup>a</sup>   |
| Mean fatigue, FSMC (± SD)               | 37.0 ± 17.5               | 38.9 ± 18.9 <sup>b</sup>          | 45.8 ± 22.5 <sup>b</sup> |
| Median EDSS (range)                     | 1.5 (0–5.0)               | 1.5 (0–5.0) <sup>c</sup>          | 1.5 (0–6.5) <sup>c</sup> |

Demographic and clinical characteristics of treatment-naïve patients with MS after their first demyelinating event at baseline (n = 601) and 4-year follow-up (n = 230).

<sup>a</sup>Fatigue scores (derived from MUSIC) between baseline and 4-year follow-up were not significantly different (*p* = 0.082; paired *t* test).

<sup>b</sup>Fatigue scores (derived from FSMC) between baseline and 4-year follow-up were significantly different (*p* < 0.001; paired *t* test) with higher values at follow-up.

<sup>c</sup>EDSS between baseline and 4-year follow-up were significantly different (*p* = 0.029; Wilcoxon signed-rank test) with higher values at follow-up.

CIS = clinically isolated syndrome; EDSS = Expanded Disability Status Scale; FSMC = Fatigue Scale for Motor and Cognitive functions; MRI = magnetic resonance imaging; MS = multiple sclerosis; MUSIC = Multiple Sclerosis Inventory of Cognition; RRMS = relapsing–remitting multiple sclerosis.

| Subcortical brain region     | Fatigue (MUSIC)<br>(baseline) |       | Fatigue (FSMC)<br>(baseline) |       | EDSS<br>(baseline) |       | Fatigue (MUSIC)<br>(4-year follow-up) |       | Fatigue (FSMC)<br>(4-year follow-up) |       | EDSS<br>(4-year follow-up) |       |
|------------------------------|-------------------------------|-------|------------------------------|-------|--------------------|-------|---------------------------------------|-------|--------------------------------------|-------|----------------------------|-------|
|                              | s                             | p     | s                            | p     | s                  | p     | s                                     | p     | s                                    | p     | s                          | p     |
|                              |                               |       |                              |       |                    |       |                                       |       |                                      |       |                            |       |
| Caudate (left)               | 0.713                         | 0.005 | 0.763                        | 0.003 | 0.772              | 0.003 | 0.691                                 | 0.003 | 0.641                                | 0.002 | 0.690                      | 0.007 |
| Caudate (right)              | 0.705                         | 0.009 | 0.755                        | 0.006 | 0.771              | 0.006 | 0.667                                 | 0.005 | 0.617                                | 0.005 | 0.685                      | 0.008 |
| Putamen (left)               | 0.639                         | 0.001 | 0.614                        | 0.002 | 0.348              | n.s.  | 0.608                                 | 0.012 | 0.603                                | 0.012 | 0.335                      | n.s.  |
| Putamen (right)              | 0.494                         | 0.012 | 0.606                        | 0.003 | 0.644              | 0.006 | 0.166                                 | n.s.  | 0.116                                | n.s.  | 0.555                      | 0.012 |
| Pallidum (left)              | 0.442                         | n.s.  | 0.606                        | 0.012 | 0.460              | n.s.  | 0.654                                 | 0.013 | 0.660                                | 0.012 | 0.607                      | 0.009 |
| Pallidum (right)             | 0.218                         | n.s.  | 0.606                        | 0.012 | 0.222              | n.s.  | 0.643                                 | 0.014 | 0.609                                | 0.013 | 0.605                      | 0.011 |
| Thalamus (left)              | 0.265                         | n.s.  | 0.215                        | n.s.  | 0.653              | 0.009 | 0.189                                 | n.s.  | 0.139                                | n.s.  | 0.606                      | 0.016 |
| Thalamus (right)             | 0.633                         | 0.001 | 0.606                        | 0.002 | 0.346              | n.s.  | 0.608                                 | 0.013 | 0.603                                | n.s.  | 0.316                      | n.s.  |
| Hippocampus (left)           | 0.500                         | 0.012 | 0.606                        | 0.003 | 0.635              | 0.001 | 0.124                                 | n.s.  | 0.074                                | n.s.  | 0.151                      | n.s.  |
| Hippocampus (right)          | 0.409                         | n.s.  | 0.359                        | n.s.  | 0.404              | n.s.  | 0.345                                 | n.s.  | 0.295                                | n.s.  | 0.269                      | n.s.  |
| Pons                         | 0.630                         | 0.001 | 0.680                        | n.s.  | 0.656              | 0.008 | 0.610                                 | 0.014 | 0.605                                | 0.013 | 0.605                      | 0.011 |
| Medulla                      | 0.165                         | n.s.  | 0.606                        | 0.012 | 0.217              | n.s.  | 0.025                                 | n.s.  | 0.607                                | 0.013 | 0.092                      | n.s.  |
| Brainstem                    | 0.416                         | n.s.  | 0.606                        | 0.012 | 0.425              | n.s.  | 0.345                                 | n.s.  | 0.295                                | n.s.  | 0.336                      | n.s.  |
| Amygdala (left)              | 0.407                         | n.s.  | 0.357                        | n.s.  | 0.390              | n.s.  | 0.337                                 | n.s.  | 0.287                                | n.s.  | 0.246                      | n.s.  |
| Amygdala (right)             | 0.258                         | n.s.  | 0.208                        | n.s.  | 0.310              | n.s.  | 0.159                                 | n.s.  | 0.109                                | n.s.  | 0.134                      | n.s.  |
| Accumbens area (left)        | 0.383                         | n.s.  | 0.333                        | n.s.  | 0.387              | n.s.  | 0.292                                 | n.s.  | 0.242                                | n.s.  | 0.216                      | n.s.  |
| Accumbens area (right)       | 0.380                         | n.s.  | 0.330                        | n.s.  | 0.366              | n.s.  | 0.270                                 | n.s.  | 0.220                                | n.s.  | 0.195                      | n.s.  |
| Ventral diencephalon (left)  | 0.039                         | n.s.  | 0.011                        | n.s.  | 0.021              | n.s.  | 0.090                                 | n.s.  | 0.060                                | n.s.  | 0.094                      | n.s.  |
| Ventral diencephalon (right) | 0.047                         | n.s.  | 0.097                        | n.s.  | 0.071              | n.s.  | 0.073                                 | n.s.  | 0.077                                | n.s.  | 0.057                      | n.s.  |
| Superior cerebellar peduncle | 0.092                         | n.s.  | 0.042                        | n.s.  | 0.057              | n.s.  | 0.058                                 | n.s.  | 0.092                                | n.s.  | 0.057                      | n.s.  |
| Midbrain                     | 0.023                         | n.s.  | 0.073                        | n.s.  | 0.021              | n.s.  | 0.091                                 | n.s.  | 0.059                                | n.s.  | 0.088                      | n.s.  |



**FIGURE 1: Subcortical brain regions: Structural equation modeling (SEM) results of the cross-sectional ( $n = 601$ ) and longitudinal ( $n = 230$ ) MS cohort. Association between 21 subcortical brain volumes and fatigue (subscale of MUSIC and FSMC) and EDSS scores at baseline and at 4-year follow-up. Significant associations are colored in the table to express the strength of significant associations between the variables (standardized coefficient =  $s$ ). Hotter colors indicate a stronger association. EDSS = Expanded Disability Status Scale; FSMC = Fatigue Scale for Motor and Cognitive functions; MS = multiple sclerosis; MUSIC = Multiple Sclerosis Inventory of Cognition; n.s. = not significant;  $s$  = standardized coefficients.**

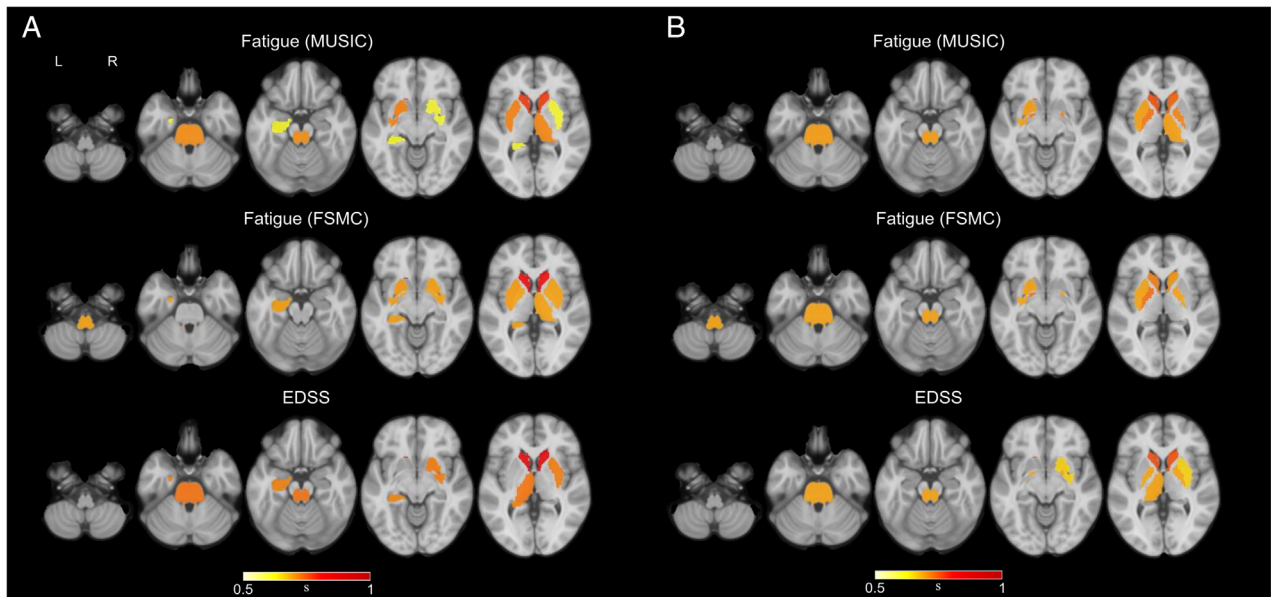


**FIGURE 2: Structural determinants of fatigue and EDSS at (A) baseline ( $n = 601$ ) and (B) at 4-year follow-up ( $n = 230$ ). Strength of association between brain structures and fatigue (measured by MUSIC and FSMC) and EDSS is expressed as standardized coefficients ( $s$ ) (color bar ranging from 0.5 to 1; the closer to 1 the stronger the association) and projected on axial brain slices. Highlighted regions are significant after multiple comparison correction. EDSS = Expanded Disability Status Scale; FSMC = Fatigue Scale for Motor and Cognitive functions; MUSIC = Multiple Sclerosis Inventory of Cognition.**

contralateral analogous structures did not reach the level of statistical significance. Fatigue measured by FSMC showed an additional association with the bilateral pallidum, medulla, and brainstem.

The baseline volumes of bilateral caudate and pons were associated with clinical disability at disease onset as measured by EDSS (all standardized coefficients [ $s$ ]  $>0.5$ , all  $p < 0.05$ ). Unilaterally, the volumes of right putamen,



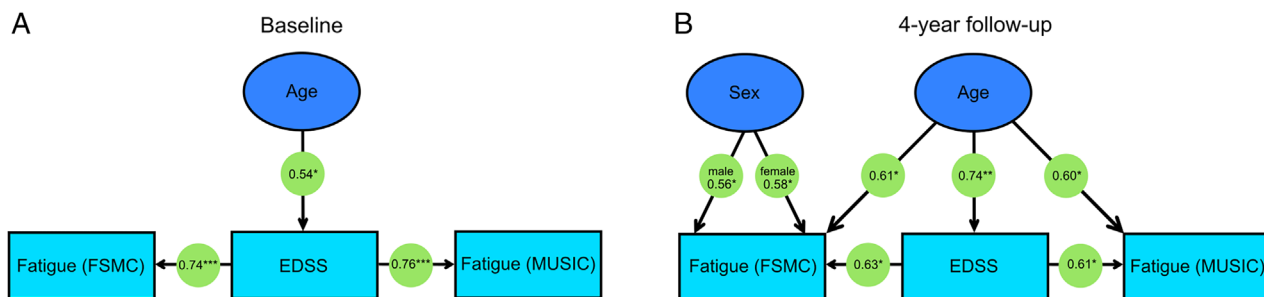


**FIGURE 3: Structural equation modeling (SEM) of demographic and clinical variables at (A) baseline ( $n = 601$ ) and (B) at 4-year follow-up ( $n = 230$ ). Arrows denote the relationship between the variables expressed as standardized coefficients, which are shown for each path (\* significant at  $p < 0.01$ ; \*\* significant at  $p < 0.001$ ; \*\*\* significant at  $p < 0.0001$ ). EDSS = Expanded Disability Status Scale; FSMC = Fatigue Scale for Motor and Cognitive functions; MUSIC = Multiple Sclerosis Inventory of Cognition.**

left thalamus, and left hippocampus were associated with EDSS (see Figs 1 and 2A); none of the contralateral analogues were associated with EDSS.

With regard to the 68 cortical regions, only the right caudal middle frontal cortex was associated with fatigue severity measured by the FSMC in the cross-sectional approach. All remaining cortical regions demonstrated no association with MUSIC, FSMC, or EDSS in the SEM (Supplementary Table S3).

Finally, neither subcortical (Supplementary Table S4) nor cortical (Supplementary Table S5) volumes were associated with fatigue measured by MUSIC and FSMC within the control cohort.

### Subcortical Volumes Predict Fatigue and Clinical Impairment after 4 Years

With regard to the functional impairment after a clinical follow-up of 4 years within the subcohort of 230 patients (second SEM model), baseline volumes of the following structures strongly predicted the 4-year follow-up scores of fatigue (measured by MUSIC and FSMC) and EDSS in descending order: bilateral caudate (all  $s > 0.6$ ), bilateral pallidum (all  $s > 0.5$ ), and pons (all  $s > 0.5$ ; see Fig 1 and 2B). Whereas both fatigue scales (MUSIC and FSMC) were predicted by SEM (in addition to the above-mentioned) by the left putamen, the EDSS was additionally predicted by the left thalamus and the right putamen (all standardized coefficients [ $s$ ]  $> 0.5$ , all  $p < 0.05$ ).

None of the cortical regions showed a significant predictive association in the longitudinal approach (see Supplementary Table S3).

### EDSS Is Associated with Baseline Fatigue

Within the third SEM model, we explored the association between age and sex with the 3 clinical variables (MUSIC, FSMC, and EDSS). In the cohort of 601 patients, age at disease onset was associated with baseline EDSS ( $s = 0.54$ ,  $p < 0.05$ ) and EDSS was associated with

baseline fatigue scores (MUSIC:  $s = 0.76$ ,  $p < 0.0001$  and FSMC:  $s = 0.74$ ,  $p < 0.0001$ ; Fig 3).

### Age, Sex, and EDSS Predict Follow-Up Fatigue

In the 4-year follow-up cohort of 230 patients (fourth SEM model), strong associations between age at disease onset and baseline EDSS ( $s = 0.74$ ,  $p < 0.001$ ) and fatigue scores (MUSIC:  $s = 0.60$ ,  $p < 0.01$  and FSMC:  $s = 0.61$ ,  $p < 0.01$ ) were detected. Baseline EDSS as well predicted both fatigue measures (MUSIC:  $s = 0.61$ ,  $p < 0.01$  and FSMC:  $s = 0.63$ ,  $p < 0.01$ ; see Fig 3). Additionally, male (FSMC:  $s = 0.56$ ,  $p < 0.01$ ) and female (FSMC:  $s = 0.58$ ,  $p < 0.01$ ) sex predicted the 4-year follow-up fatigue within this SEM model.

### Network Hubs Colocalize with Structural Determinants of Fatigue and Disability

Within the reconstructed structural covariance network, we defined network hubs based on the betweenness centrality measure. These hub regions are generally characterized by their central placement in the overall architecture of a network. Patients with MS with progression in fatigue based on the MUSIC score over 4 years were found to show network hubs in the bilateral pallidum ( $p = 0.007$  [left];  $p = 0.006$  [right]), pons ( $p = 0.0001$ ) and brainstem ( $p = 0.005$ ). Patients with progression in fatigue based on the FSMC score showed network hubs in the bilateral putamen ( $p = 0.008$  [left];  $p = 0.007$  [right]), pons ( $p = 0.0001$ ), and brainstem ( $p = 0.006$ ). No hubs were detected in patients with fatigue-stable MS (neither with MUSIC nor with FSMC scores). Patients with EDSS worsening after 4 years demonstrated brain network hubs in the bilateral caudate ( $p = 0.009$  [left] and  $p = 0.008$  [right]), pons ( $p = 0.003$ ), and brainstem ( $p = 0.004$ ). Finally, patients with clinically stable MS (no EDSS worsening) revealed no network hubs. The above-mentioned  $p$  values were FDR corrected.



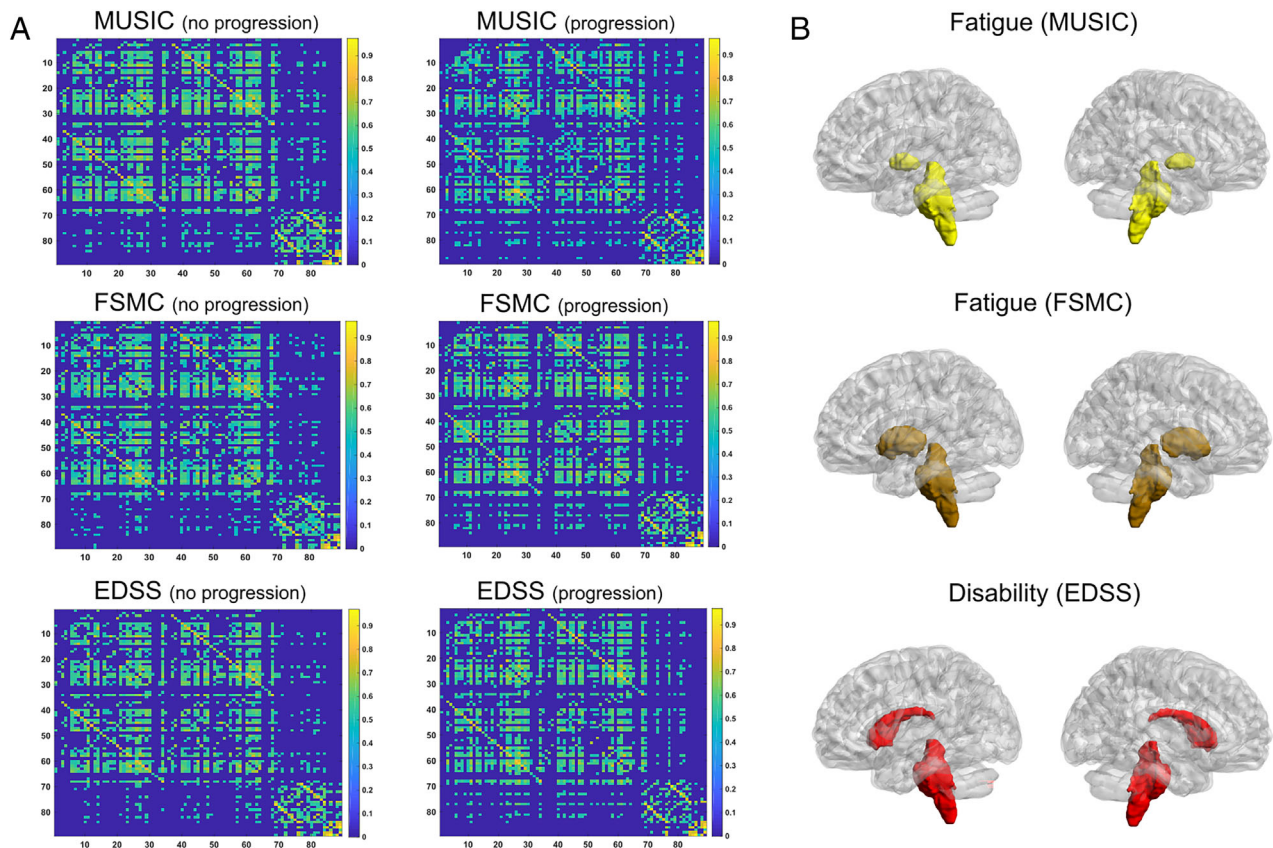


**FIGURE 4: Matrices (A) and network hubs (B) from structural covariance network (SCN) analysis. (A)** In the covariance matrices (size  $89 \times 89$ ), each element represents Pearson's correlation coefficient between regions of interest values across subjects in one group. **(B)** Brain network hubs (significant regions from the SCN analysis) in patients with MUSIC, FSMC, and EDSS progression in the 4-year longitudinal study cohort ( $n = 230$ ). EDSS = Expanded Disability Status Scale; FSMC = Fatigue Scale for Motor and Cognitive functions; MUSIC = Multiple Sclerosis Inventory of Cognition.

The regions that emerged as network hubs in patients who experienced progression are visualized in Figure 4.

## Discussion

In this study, we obtained volumes from cortical and subcortical brain structures to evaluate the structure–function association of fatigue in the initial stages of the disease in a large cohort of patients with MS. Our findings showed a strong association between the caudate and pons volumes and fatigue scores at disease onset. Predictive causal modeling through SEM confirmed that the caudate and pons volumes were also significant determinants that influence fatigue development in MS over time. Our covariance network analysis of subcortical morphology demonstrated that these subcortical regions further colocalized with structural network hubs in those patients with progressing fatigue. These hubs were absent in patients with stable scores.

Our initially untreated cohort allows a direct view of clinical–volumetric associations in the very initial stages of

the disease. From this cohort, 230 patients were clinically followed up for a mean of 4 years to determine baseline volumetric structures that best predict fatigue and EDSS worsening over time. Our clinical follow-up findings demonstrated that in addition to caudate and pons (both of which were associated with the baseline characteristics) the bilateral pallidum volumes strongly predicted future fatigue as well as EDSS.

This association of exclusively subcortical GM structures measured at onset and fatigue suggests a prominent role of these brain regions in terms of fatigue evolution in the initial stages of the disease and probably even in a prodromal phase of the disease.

Clinical impairment in MS is characterized by neurological and neuropsychological disability that shows robust associations with brain atrophy<sup>43</sup> and GM pathology.<sup>44</sup> However, GM alterations are not uniform across all brain structures, as some regions are more susceptible to atrophy than others.<sup>45,46</sup> A recent longitudinal study reported that atrophy of DGM structures (caudate, pallidum, and putamen) possesses a pivotal role in predicting

disability accrual over time in different MS subtypes.<sup>47</sup> In addition, the DGM structures showed the fastest annual rate of volume loss in patients with a relapse onset.<sup>47</sup> Moreover, the sequence of atrophy progression in the relapsing–remitting and progressive forms of the disease is comparable, although the cerebellum, caudate, and putamen show an earlier atrophy in patients with RRMS.<sup>48</sup> Our results extend these observations by demonstrating that volume reduction of these DGM structures is associated with concomitant and future fatigue progression to a similar extent as clinical disability measured by the EDSS in an initially treatment-naïve cohort.

In addition to the structural alterations seen here, a framework of neuronal activity and functional connectivity typical of MS-related fatigue has been developed in recent years.<sup>23</sup> The primarily functional neural origin of fatigue includes alterations of the dynamic connectivity between hemispheric sensorimotor regions, of the resting-state connectivity within the default mode network and of the striatum and its projections.<sup>23</sup> One possible explanation for altered connectivity is that networks mediating specific cognitive operations are perturbed by the observed DGM structural damage leading to functional reorganization even distant from the primary site of injury by rearranging the entire brain network.<sup>4</sup>

Even though fatigue is clinically well-characterized, the underlying pathophysiological mechanisms remain incompletely understood.<sup>4</sup> This might be traced back to mixed (mainly inconsistent) results on the potential link between global measures of brain atrophy and fatigue.<sup>49,50</sup> One study has demonstrated the association between lower global GM fraction and fatigue,<sup>49</sup> whereas another has postulated that scattered regional damage contributes more to fatigue than global brain damage.<sup>51</sup> Moreover, it has recently been demonstrated that fatigue is also related to widespread normal-appearing WM damage and to a lesser extent to conventional lesion load or GM atrophy.<sup>13</sup> However, specific brain regions seem to be typically involved in the development of fatigue.<sup>10</sup>

Our results suggest that patients with MS with caudate and pallidal atrophy develop progressing fatigue, and thus might reveal less premorbid functional reserve or reduced resistance to atrophy. In fact, fatigue-related records were found with higher frequency among patients with MS than controls up to 5 years before the clinical onset in a large registry study.<sup>6</sup>

Our additional network analysis approach has consistently identified the same DGM structures linked to fatigue and clinical progression as in the conventional volumetric analysis. The occurrence of network hubs within the putamen, pallidum, caudate, and pons in patients experiencing progression (but not in stable patients) may

be indicative of disturbances in DGM's local physiology, energy metabolism, and neural processing that set them apart from other, less-central brain network regions. The colocalization of the hubs to the subcortical structures (putamen, caudate, pallidum, and pons) identified in the main analysis could reflect the subcortical network's response to early tissue damage through structural reorganization.<sup>52</sup> Acting as an integrative hub of upstream and downstream information flow, the early affection of the striatum might precipitate the “emersion” of fatigue and clinical disability.

Interestingly, the thalamus volume at disease onset displayed a less consistent pattern in predicting clinical impairment. Its atrophy appears to represent a common pathway through which both WM lesions and focal DGM pathology contribute to clinical disability.<sup>53</sup> However, among the subcortical structures, our data attribute caudate and pallidum a stronger predictive validity in fatigue progression than the thalamus. This finding could be partly supported by the functional implications of striatum in self-motivation and reward-related components of fatigue, and the decrement in motivational influence from the striatal inputs to the frontal lobe would aggravate expression of fatigue.<sup>4</sup>

Our third predictive model (including only demographics and the clinical scores) is notable for at least 3 main features. First, age is associated with disease severity measured by the EDSS at disease onset and additionally with EDSS and both fatigue scores in the 4-year follow-up cohort, confirming interdependency between these variables. Second, this model provides causal evidence of an association between physical disability itself (EDSS) and both fatigue measures in the baseline as well as the 4-year follow-up cohort. Third, it demonstrates that both men and women were significant determinants that influence fatigue (measured by FSMC), consistent with some observations having shown that women and men experience MS-related fatigue with the same frequency.<sup>54</sup>

In conclusion, our findings provide evidence that early fatigue is related to DGM integrity loss at disease onset in a large cohort of initially untreated patients with MS. Subcortical volume reductions, mainly within the caudate, pallidum, and pons, are important scaffolds in predicting emerging fatigue. Our model-based approaches went beyond correlation analysis and investigated associations quantifying the pathways underlying fatigue development and subcortical brain volume changes. Finally, the colocalization of the detected subcortical regions with structural network hubs in patients with progressing fatigue suggests an integrating role of these brain regions in terms of fatigue evolution. These observations should urge close follow-up of high-risk patients for fatigue

worsening, encourage clinical decisions already from the disease onset and thereby reduce the burden of progressing fatigue.

## Acknowledgments

The authors thank Cheryl Ernest for proofreading the manuscript. We also thank Lena Minch for her technical assistance. Some results presented here are part of her MD thesis. The German National MS cohort and KKNMS are supported by grants from the German Federal Ministry for Education and Research (BMBF), grant no. 01GI0914 (Bochum), 01GI0916, 01GI1601G (Lübeck), and 01GI1601B (Marburg). This work was also supported by the German Research Foundation (DFG) SFB CRC-TR 128. Open Access funding enabled and organized by Projekt DEAL.

## Author Contributions

Conception and design of the study: V.F., F.Z., S.G., and M.M. Data acquisition, analysis and interpretation: all authors. Statistical analysis: V.F. and M.M. Drafting of the manuscript: V.F., D.C., G.G.-E., F.Z., S.G., and M.M. Revising the manuscript: all authors.

## Potential Conflicts of Interest

The authors report no relevant conflicts of interest.

## References

- Siffrin V, Vogt J, Radbruch H, et al. Multiple sclerosis–candidate mechanisms underlying CNS atrophy. *Trends Neurosci* 2010;33:202–210.
- von Bismarck O, Dankowski T, Ambrosius B, et al. Treatment choices and neuropsychological symptoms of a large cohort of early MS. *Neurol Neuroimmunol Neuroinflamm* 2018;5:e446.
- Lerdal A, Celius EG, Krupp L, Dahl AA. A prospective study of patterns of fatigue in multiple sclerosis. *Eur J Neurol* 2007;14:1338–1343.
- Manjaly Z-M, Harrison NA, Critchley HD, et al. Pathophysiological and cognitive mechanisms of fatigue in multiple sclerosis. *J Neurol Neurosurg Psychiatry* 2019;90:642–651.
- Runia TF, Jafari N, Siepmann DA, Hintzen RQ. Fatigue at time of CIS is an independent predictor of a subsequent diagnosis of multiple sclerosis. *J Neurol Neurosurg Psychiatry* 2015;86:543–546.
- Disanto G, Zecca C, MacLachlan S, et al. Prodromal symptoms of multiple sclerosis in primary care. *Ann Neurol* 2018;83:1162–1173.
- Cortese M, Riise T, Bjørnevik K, et al. Preclinical disease activity in multiple sclerosis: a prospective study of cognitive performance prior to first symptom. *Ann Neurol* 2016;80:616–624.
- Chalah MA, Riachi N, Ahdab R, et al. Fatigue in multiple sclerosis: neural correlates and the role of non-invasive brain stimulation. *Front Cell Neurosci* 2015;9:460.
- Sepulcre J, Masdeu J, Goni J, et al. Fatigue in multiple sclerosis is associated with the disruption of frontal and parietal pathways. *Mult Scler J* 2009;15:337–344.
- Calabrese M, Rinaldi F, Grossi P, et al. Basal ganglia and frontal/parietal cortical atrophy is associated with fatigue in relapsing-remitting multiple sclerosis. *Mult Scler* 2010;16:1220–1228.
- Willing J, Rolfsnes HO, Zimmermann H, et al. Structural correlates for fatigue in early relapsing remitting multiple sclerosis. *Eur Radiol* 2016;26:515–523.
- Damasceno A, Damasceno BP, Cendes F. Atrophy of reward-related striatal structures in fatigued MS patients is independent of physical disability. *Mult Scler J* 2016;22:822–829.
- Novo AM, Batista S, Alves C, et al. The neural basis of fatigue in multiple sclerosis: a multimodal MRI approach. *Neurol Clin Pract* 2018;8:492–500.
- Rocca MA, Agosta F, Colombo B, et al. fMRI changes in relapsing-remitting multiple sclerosis patients complaining of fatigue after IFNbeta-1a injection. *Hum Brain Mapp* 2007;28:373–382.
- Rocca MA, Meani A, Riccitelli GC, et al. Abnormal adaptation over time of motor network recruitment in multiple sclerosis patients with fatigue. *Mult Scler* 2016;22:1144–1153.
- Biseco A, Nardo FD, Docimo R, et al. Fatigue in multiple sclerosis: the contribution of resting-state functional connectivity reorganization. *Mult Scler* 2018;24:1696–1705.
- Jaeger S, Paul F, Scheel M, et al. Multiple sclerosis-related fatigue: altered resting-state functional connectivity of the ventral striatum and dorsolateral prefrontal cortex. *Mult Scler* 2019;25:554–564.
- Finke C, Schlichting J, Papazoglou S, et al. Altered basal ganglia functional connectivity in multiple sclerosis patients with fatigue. *Mult Scler* 2015;21:925–934.
- Filippi M, Rocca MA, Colombo B, et al. Functional magnetic resonance imaging correlates of fatigue in multiple sclerosis. *Neuroimage* 2002;15:559–567.
- Fleischer V, Muthuraman M, Anwar AR, et al. Continuous reorganization of cortical information flow in multiple sclerosis: a longitudinal fMRI effective connectivity study. *Sci Rep* 2020;10:806.
- Rocca MA, Valsasina P, Colombo B, et al. Cortico-subcortical functional connectivity modifications in fatigued multiple sclerosis patients treated with fampridine and amantadine. *Eur J Neurol* 2021;28:2249–2258.
- Chaudhuri A, Behan PO. Fatigue in neurological disorders. *Lancet* 2004;363:978–988.
- Bertoli M, Tecchio F. Fatigue in multiple sclerosis: does the functional or structural damage prevail? *Mult Scler* 2020;26:1809–1815.
- Svenningsson A, Falk E, Celius EG, et al. Natalizumab treatment reduces fatigue in multiple sclerosis. Results from the TYNERGY trial; a study in the real life setting. *PLoS One* 2013;8:e58643.
- Barkhof F, Filippi M, Miller DH, et al. Comparison of MRI criteria at first presentation to predict conversion to clinically definite multiple sclerosis. *Brain* 1997;120:2059–2069.
- Polman CH, Reingold SC, Banwell B, et al. Diagnostic criteria for multiple sclerosis: 2010 revisions to the McDonald criteria. *Ann Neurol* 2011;69:292–302.
- Johnen A, Bürkner P-C, Landmeyer NC, et al. Can we predict cognitive decline after initial diagnosis of multiple sclerosis? Results from the German National early MS cohort (KKNMS). *J Neurol* 2018;1-12:386–397.
- Calabrese P, Kalbe E, Kessler J. Ein neuropsychologisches Screening zur Erfassung kognitiver Störungen bei MS-Patienten-Das Multiple Sklerose Inventarium Cognition (MUSIC). *Psychoneuroendocrinology* 2004;30:384–388.
- Penner I, Raselli C, Stöcklin M, et al. The fatigue scale for motor and cognitive functions (FSMC): validation of a new instrument to assess multiple sclerosis-related fatigue. *Mult Scler J* 2009;15:1509–1517.
- Elbers RG, Rietberg MB, van Wegen EE, et al. Self-report fatigue questionnaires in multiple sclerosis, Parkinson's disease and stroke: a systematic review of measurement properties. *Qual Life Res* 2012;21:925–944.

31. Sacco R, Santangelo G, Stamenova S, et al. Psychometric properties and validity of beck depression inventory II in multiple sclerosis. *Eur J Neurol* 2016;23:744–750.
32. Schmidt P, Gaser C, Arsic M, et al. An automated tool for detection of FLAIR-hyperintense white-matter lesions in multiple sclerosis. *Neuroimage* 2012;59:3774–3783.
33. Fischl B. FreeSurfer. *Neuroimage* 2012;62:774–781.
34. Desikan RS, Ségonne F, Fischl B, et al. An automated labeling system for subdividing the human cerebral cortex on MRI scans into gyral based regions of interest. *Neuroimage* 2006;31:968–980.
35. Kelley K, Lai K. Accuracy in parameter estimation for the root mean square error of approximation: sample size planning for narrow confidence intervals. *Multivar Behav Res* 2011;46:1–32.
36. Tzourio-Mazoyer N, Landeau B, Papathanassiou D, et al. Automated anatomical labeling of activations in SPM using a macroscopic anatomical parcellation of the MNI MRI single-subject brain. *Neuroimage* 2002;15:273–289.
37. Ellison GW, Myers LW, Leake BD, et al. Design strategies in multiple sclerosis clinical trials. The Cyclosporine Multiple Sclerosis Study Group. *Ann Neurol* 1994;36:S108–S112.
38. Hosseini SM, Hoefft F, Kesler SR. GAT: a graph-theoretical analysis toolbox for analyzing between-group differences in large-scale structural and functional brain networks. *PLoS One* 2012;7:e40709.
39. Rubinov M, Sporns O. Complex network measures of brain connectivity: uses and interpretations. *Neuroimage* 2010;52:1059–1069.
40. van den Heuvel MP, Sporns O. Network hubs in the human brain. *Trends Cogn Sci* 2013;17:683–696.
41. Genovese CR, Lazar NA, Nichols T. Thresholding of statistical maps in functional neuroimaging using the false discovery rate. *Neuroimage* 2002;15:870–878.
42. Smith CE, Cribbie RA. Multiplicity control in structural equation modeling: incorporating parameter dependencies. *Struct Equ Modeling* 2013;20:79–85.
43. Popescu V, Agosta F, Hulst HE, et al. Brain atrophy and lesion load predict long term disability in multiple sclerosis. *J Neurol Neurosurg Psychiatry* 2013;84:1082–1091.
44. Geurts JJ, Calabrese M, Fisher E, Rudick RA. Measurement and clinical effect of grey matter pathology in multiple sclerosis. *Lancet Neurol* 2012;11:1082–1092.
45. Steenwijk MD, Geurts JJ, Daams M, et al. Cortical atrophy patterns in multiple sclerosis are non-random and clinically relevant. *Brain* 2016;139:115–126.
46. Preziosa P, Pagani E, Mesaros S, et al. Progression of regional atrophy in the left hemisphere contributes to clinical and cognitive deterioration in multiple sclerosis: a 5-year study. *Hum Brain Mapp* 2017;38:5648–5665.
47. Eshaghi A, Prados F, Brownlee WJ, et al. Deep gray matter volume loss drives disability worsening in multiple sclerosis. *Ann Neurol* 2018;83:210–222.
48. Eshaghi A, Marinescu RV, Young AL, et al. Progression of regional grey matter atrophy in multiple sclerosis. *Brain* 2018;141:1665–1677.
49. Tedeschi G, Dinacci D, Lavorgna L, et al. Correlation between fatigue and brain atrophy and lesion load in multiple sclerosis patients independent of disability. *J Neurol Sci* 2007;263:15–19.
50. Marrie RA, Fisher E, Miller DM, et al. Association of fatigue and brain atrophy in multiple sclerosis. *J Neurol Sci* 2005;228:161–166.
51. Rocca MA, Parisi L, Pagani E, et al. Regional but not global brain damage contributes to fatigue in multiple sclerosis. *Radiology* 2014;273:511–520.
52. Fleischer V, Radetz A, Ciolac D, et al. Graph theoretical framework of brain networks in multiple sclerosis: a review of concepts. *Neuroscience* 2019;403:35–53.
53. Azevedo CJ, Cen SY, Khadka S, et al. Thalamic atrophy in multiple sclerosis: a magnetic resonance imaging marker of neurodegeneration throughout disease. *Ann Neurol* 2018;83:223–234.
54. Bakshi R. Fatigue associated with multiple sclerosis: diagnosis, impact and management. *Mult Scler* 2003;9:219–227.